Development and Characterization of Soil Material Parameters for Embankment Breach

G. J. Hanson, D. M. Temple, S. L. Hunt, R. D. Tejral

Abstract. *Despite the widespread use of earthen dams, the processes by which earthen embankments erode and fail when overtopped during extreme events are only imperfectly understood. Aging of these dams and the associated recent focus on dam rehabilitation has increased the need for new technology and tools for predicting the performance of earthen embankments during overtopping. Windows Dam Analysis Modules (WinDAM B) is a modular software application being developed to address this need for homogeneous earthen embankments. This software is being developed through joint efforts of the Agricultural Research Service, the Natural Resources Conservation Service, and Kansas State University. The computational model being incorporated into this software is the result of research including embankment overtopping tests conducted in the outdoor laboratory. The WinDAM B model is a simplified representation of the observed process of progressive erosion leading to embankment breach to be useful for field application the model has been developed to utilize soil parameters that may be reasonably obtained for the conditions to which the model is applied. This article presents the background for the material parameter input requirements for overtopping erosion and breach analysis including: 1) the detachment rate coefficient and critical stress parameters of the excess stress equation, 2) the total unit weight of soil, 3) the undrained shear strength, and 4) the headcut migration coefficient.*

Keywords. *Dams, Breach, Failure, Process, Model, Erosion, Erodibility, Density, Strength, Headcut.*

The study of 18 historical cases of embankment dam failures by Walder and O'Connor (1997) provides some insight into the rate of embankment erosion and breach failure. The mean vertical erosion rate parameter (k) that they used for overtopping was based on dam height divided by breach formation time. The k value in the 18 historical cases was determined to range from 1 to 1000 m-h^{-1}. That study pointed out the importance of the rate of failure in determining the peak discharge. The shortcoming of the k parameter as defined by Walder and O'Connor is that it is not related to the varying erosion processes observed during breach failure and it does not separate material property effects from geometry or hydraulic effects. In order for future modeling to address the appropriate rates, it is necessary to provide algorithms appropriate for the key erosion processes that include rate parameters that separate material property effects from geometry and hydraulic effects.

Ralston (1987) states that in the few historical cases that have been observed, the critical erosion process in embankment dam breach for cohesive embankments is headcut formation and advance. A headcut has been defined as a nearly vertical drop in channel bed elevation. For cohesive soil embankments, overtopping can lead to eventual degradation of the surface of the downstream slope of the embankment, formation of a discontinuity, and development of an overfall or headcut. Once formed, the headcut advances progressively headward as the base of the headcut deepens and widens. Failure and breach occur when the headcut migrates through the upstream crest of the dam. Therefore, headcut development and advance is a very important erosion process in determining the time of breach initiation and formation.

In addition to historical cases, observations from recent embankment overtopping research studies of cohesive materials (Hassan et al., 2004; Vaskinn et al., 2004; Hanson et al., 2005a), even though at different scales, still confirm headcutting as a key erosion process during overtopping. Hassan et al. (2004) conducted overtopping tests on six 0.6-m high clay embankments. The overtopping research reported by Vaskinn et al. (2004) involved testing of a 6-m high clay embankment. Hanson et al. (2005a) conducted overtopping tests on seven 1.3- to 2.3-m high embankments with three soil materials ranging from sandy clay to clay loam. The erosion mechanics for the three soils tested, although different in rate, were similar in process.

For purposes of discussion and evaluation, Hanson et al. (2005a) divided the observed breach process during overtopping into four stages of erosion (fig. 1): Stage 1 - headcut formation on the downstream slope (i.e. surface failure) (Phase 1) and discontinuity development (Phase 2); Stage 2 - headcut advance through the embankment crest, Stage 3 - breach formation as the headcut enters the reservoir; and Stage 4 - breach expansion/widening during reservoir drawdown. The current WinDAM B (Windows Dam Analysis Modules B) model under development for embankment breach analysis assumes a homogeneous cohesive embankment and incorporates these four stages in defining the

Submitted for review in August 2010 as manuscript number SW 8749; approved for publication by the Soil & Water Division of ASABE in March 2011.

The authors are **Gregory J. Hanson, ASABE Member Engineer,** Research Leader, **Darrel M. Temple, ASABE Member Engineer,** Research Hydraulic Engineer (retired), **Sherry L. Hunt, ASABE Member Engineer,** Research Hydraulic Engineer, and **Ronald D. Tejral, ASABE Member Engineer,** Agricultural Engineer, USDA-ARS-HERU, Stillwater, Oklahoma. **Corresponding author:** Gregory J. Hanson, USDA-ARS-HERU, 1301 N. Western, Stillwater, OK 74075; phone: 405-624-4135; e-mail: greg.hanson@ars.usda.gov.

Figure 1. Observed erosion processes during overtopping tests: (a) rills and cascade of small overfalls during stage 1, (b) consolidation of small overfalls during stage 1, (c) headcut at downstream crest, transition from stage 1 to stage 2, (d) headcut at upstream crest, transition from stage 2 to stage 3, (e) flow through breach during stage 3, and (f) transition from stage 3 to stage 4. (Hanson et al., 2005a).

transitions that the algorithms use to quantify the breach erosion process.

A key part in modeling the erosion of embankments is characterizing the materials and their impact on the rate of erosion. Hanson et al. (2005a), in addition to observed erosion processes, also reported that soil gradation (i.e. % clay, silt and sand content) and compaction properties significantly influenced rate of the erosion processes (i.e. headcut advance and widening). They provided descriptions of the three soil materials used in the seven overtopping failure tests: Soil 1 was described as an SM (silty sand) with 5% clay and 70% sand; Soil 2 was described as an SM (silty sand) with 6% clay and 63% sand; and Soil 3 was described as a CL (lean clay) with 26% clay and 25% sand. The test embankments were constructed with equivalent lift thicknesses and compaction effort. The headcut migration (fig. 2a) and widening (fig. 2b) rates were observed to vary over several orders of magnitude and were directly linked to soil texture and compaction water content. The rates of erosion governing these processes tended to be inversely related to clay content and compaction water content.

The algorithms within WinDAM B have been developed to simulate the erosion processes of the different stages of embankment breach and to incorporate material parameters that can be reasonably obtained or estimated for the conditions to which the model is applied. The purpose of this article is to describe the material properties required as inputs to the WinDAM B model currently under development for prediction of erosion rates and provide background and methods for determining these values.

Erosion Process Algorithms

Stage 1 Phase 2 through Stage 4

A detailed description of the erosion processes modeled, algorithms used, and the accompanying assumptions for

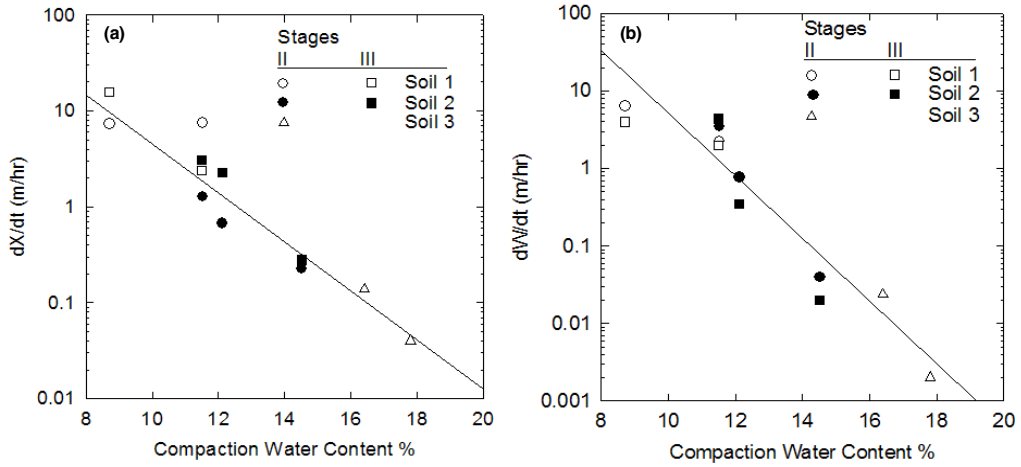

Figure 2. (a) Headcut migration rate (*dX*/*dt*), and (b) Erosion widening rate (*dW*/*dt*) vs. compaction water content (Hanson et al., 2005a).

computations of erosion during the stages modeled in WinDAM B will be provided in a future paper. The excess stress equation and headcut advance equations are the primary computation equations used for modeling the erosion processes for Stage 1 Phase 2 (discontinuity development following failure of surface protection) through Stage 4 and are described briefly here to understand the material parameters that need to be characterized for input to the WinDAM B computational model.

The excess stress equation, which is commonly used to characterize the erodibility of soil materials (Hutchinson, 1972; Foster et al., 1977; Dillaha and Beasley, 1983; Temple, 1985; Hanson, 1989; Stein and Nett, 1997; Wan and Fell, 2004) incorporates the relationship of hydraulic stress and soil erosion resistance.

$$E_r = k_d(\tau_e - \tau_c) \quad (1)$$

where

E_r = the erosion rate,
k_d = a detachment rate/erodibility coefficient,
τ_e = the hydraulically applied boundary stress, and
τ_c = the critical stress required to initiate detachment for the material.

The excess stress equation has been used in algorithms relating key erosion processes of embankment erosion including headcut jet impingement (Hanson et al., 2002), headcut migration (Hanson et al., 2001), and embankment breach widening (Hunt et al., 2005). The detachment rate coefficient k_d and critical stress τ_c are properties of the soil material. It is the intent of this article to provide background on these parameters and guidance for determination of their value for use in predicting embankment performance during overtopping.

In addition to the excess stress equation for predicting surface detachment erosion there are two algorithms within WinDAM B that are used to predict headcut advance erosion:

An energy based headcut model designated Temple/Hanson model (Temple et al., 2005):

$$dX/dt = C(qH_h)^{1/3} \quad (2)$$

where

dX/dt = the rate of headcut advance,
q = the unit discharge in the breach area,
H_h = the headcut height, and
C = an advance rate coefficient.

The advance rate coefficient is a material property and guidance for determining this property will be provided in this article. The hydraulic attack term, (qH_h), represents an approximation of the energy dissipation per unit width of overfall and C represents the material impact on the rate of headcut advance.

The energy approach has its origin in the work with spillway erosion and has been applied to embankment test data as discussed by Hanson et al. (2005b). It has the advantage of allowing the user to directly apply experience with similar conditions through calibration of the headcut advance rate coefficient entered into the model. It has the disadvantage of being more empirical than the stress-based model with the bounds of application not clearly defined due to the extremely limited validation data.

The stress-based model is more complex and less easily calibrated by the user. However, the stress model is considered to more closely represent the physical action of the erosion/failure process. Focus of the following discussion is on the stress-based model and determination of the material parameters required for its application.

A stress based headcut advance model (Hanson et al., 2001) that incorporates equation 1 as a part of equation 3:

$$\frac{dX}{dt} = \left(\frac{H_h}{2E_v}\right)k_d[\tau_e - \tau_c] \quad (3)$$

where

X = headcut location,
H_h = headcut height (fig. 3), and
E_v = erosion on the vertical face required to cause the headcut to become unstable and fail (fig. 3).

The value of E_v corresponding to the failure condition depends on relative headcut height, weight of the soil, weight of the water, tailwater depth, and soil strength. The weight of the soil and soil strength are additional soil material properties that must be determined and provided as input to the model.

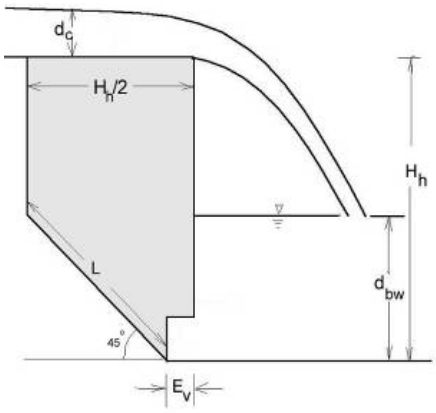

Figure 3. Schematic of head cut.

Determination of Material Parameters

The material input parameters required for WinDAM B embankment breach analysis include: 1) the erodibility parameters; detachment rate coefficient, k_d and the threshold stress, τ_c; 2) total unit weight γ_t of the embankment soil; 3) the undrained shear strength, c_u; or 4) the headcut migration rate coefficient, C. The following paragraphs provide guidance in determining each parameter.

Erodibility

Detachment Rate Coefficient k_d and Critical Stress τ_c

Several test methods have been developed for determining one or both of these parameters for the excess stress equation, including: flume tests (Smerdon and Beasley, 1959; Partheniades and Paaswell, 1968; Hanson, 1989 and 1990a), jet erosion test (JET) (Moore and Masch, 1962; Hollick, 1976; Hanson, 1990b; Hanson and Cook, 2004; Wahl et al., 2009), rotating cylinder test (RCT) (Moore and Masch, 1962; Arulanandan et al., 1973; Lim, 2006), small samples inserted in the bottom of flumes (Briaud et al., 2001, Mostafa et al., 2008), and hole erosion test (HET) (Wan and Fell, 2004; Wahl et al., 2009) are representative examples from the literature. The difficulty with these tests is that, even though they provide similar parameters, there is some question as to: 1) whether the various test methods truly provide the same measurement and values; and 2) whether the measurements are coherent with the larger scale erosion process modeled. There have been research studies conducted to address the first question by comparing the HET and RCT (Lim, 2006) and the HET and the JET (Wahl et al., 2009). There have also been studies to address the second question by comparing the JET to large-scale erosion process tests of breach widening (Hanson and Hunt, 2007), jet impingement scour (Hanson et al., 2002, 2010), and headcut migration (Hanson et al., 2001, 2010).

Lim (2006) reported that RCT measurements of erodibility resulted in values of nearly two orders of magnitude greater than the HET for non-dispersive soils and nearly a half-order of magnitude greater for dispersive soils. Wahl et al. (2009) also reported JET measurements of erodibility one to two orders of magnitude greater than HET. Although both studies concluded that the different methods produced similar relative rankings of erodibility for different soils, neither study concluded if any of the methods were coherent with larger scaled erosion processes to be modeled from test results.

Hanson and Hunt (2007) conducted a laboratory scale JET study on the impact of compaction effort and compaction water content. As part of that study they compared laboratory JET measurements of k_d to values of k_d determined from large-scale embankment breach widening tests (figs. 4 and 5). They concluded that soil texture, compaction energy, and compaction water content have a significant impact on erodibility (fig. 5) and that small-scale JET measurements were coherent with the larger scale test results.

In an effort to expand the investigation of coherence of JET measurements to larger scale erosion processes, Hanson et al. (2010) compared results from a series of compaction tests in the laboratory to large-scale erosion process flume tests on vertical overfall scour (Hanson et al., 2002) and headcut advance (Hanson et al., 2001) (figs. 6-9). The process tests were conducted in a 1.8-m wide, 29.3-m long flume, with 2.4-m high sidewalls. JET laboratory tests were conducted using the same fill material as used in the flume tests, a soil with 25% clay and a plasticity index of 15.

Figure 4. Large-scale embankment widening tests.

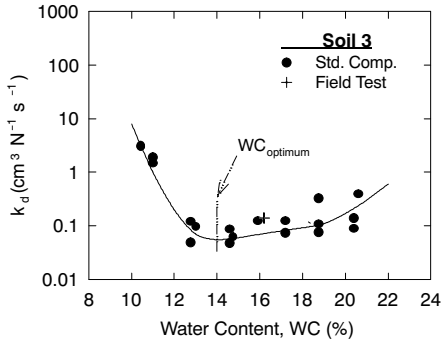

Figure 5. Large-scale field test and laboratory JET results (Hanson and Hunt, 2007).

Figure 6. Headcut scour (Hanson et al., 2002).

Figure 7. Headcut advance (Hanson et al., 2001).

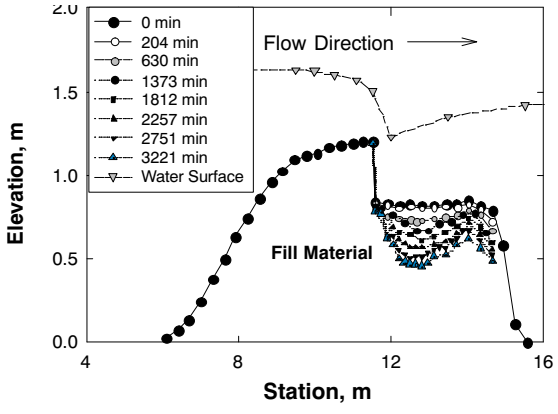

Figure 8. Observed scour for selected time intervals for test 13 (Hanson et al. 2002).

The small-scale laboratory JET tests were conducted on remolded samples prepared at various compaction water contents and three compaction efforts (figs. 10 and 11). The k_d values from the laboratory tests were compared to the k_d values determined from the flume tests, and to JET k_d values measured *in-situ* from flume test samples (fig. 11). The results showed: 1) compaction effort impacts erodibility; 2)

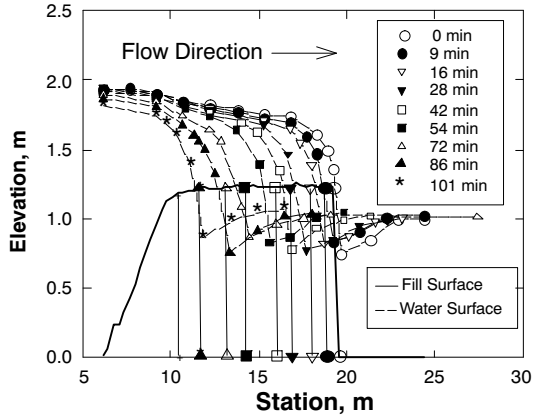

Figure 9. Observed headcut advance for selected time intervals for test 4 (Hanson et al., 2001).

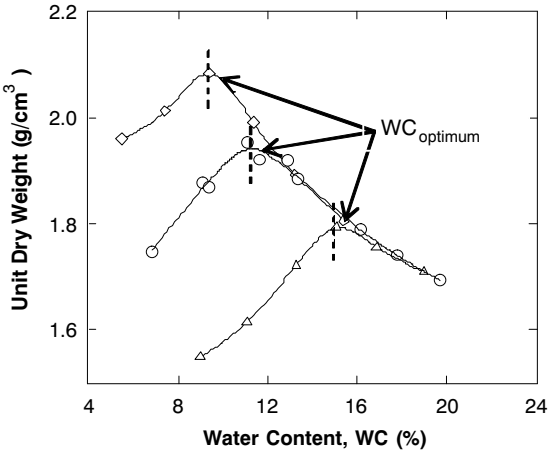

Figure 10. Comparison of compaction dry unit weight curves at three compaction efforts (27.5, 6.0, and 1.2 kg·cm/cm^3) (Hanson et al., 2010).

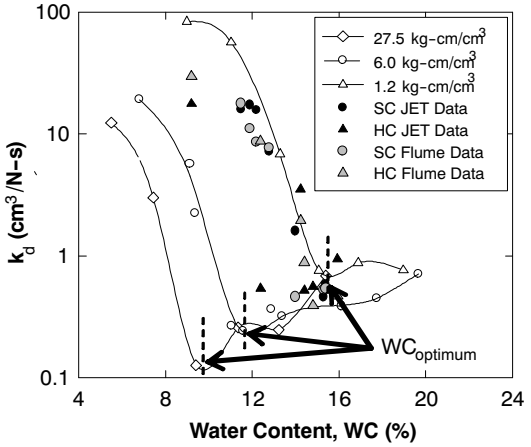

Figure 11. Coherence of k_d for large-scale erosion process test results and small-scale JET flume and laboratory sample results (Note: SC - scour tests, HC - headcut advance tests) (Hanson et al., 2010).

optimum water content produces minimum k_d values and there are very steep gradients of change in k_d on the dry side of the optimum water content for each compaction effort; 3) the gradient of change of k_d is flatter on the wet side of optimum water content; 4) the curves at different compaction

efforts join together at comparable water contents on the wet-side of optimum; and 5) the large-scale flume test results and the small-scale JET results were coherent for values of erodibility.

Details of the JET equipment, test procedures, and method of analysis are provided in Hanson and Cook (2004) and Hanson and Hunt (2007). Based on observations from erosion tests in the laboratory and field, there are many factors that impact the erodibility of a soil material and erodibility can vary over several orders of magnitude. Therefore, it is recommended that erodibility measurements be conducted on the material of interest, *in situ*, and in the hydraulic stress range of interest whenever possible.

To estimate of the range of anticipated erodibilities (k_d and τ_c) for compacted soils in earthen embankments, a series of 183 laboratory JET measurements were conducted on seven soils over a range of compaction efforts and water contents. Table 1 summarizes the soils used. Samples were compacted in the standard 101.6-mm diameter cylinder mold described in ASTM D698 (ASTM 2010) Compaction efforts applied to samples varied from 1.2 to 27.5 kg cm cm^{-3} using a 4.54-kg hammer with a 457-mm drop or a 2.49-kg hammer with a 305-mm drop. Figure 12 shows a plot of the k_d values for the seven soils at a compaction effort of 6.0 kg cm cm^{-3}. A compaction effort of 6.0 kg cm cm^{-3} is equivalent to the standard compaction prescribed in ASTM D698. The soil texture (% clay) and Plasticity Index (PI) have a strong influence on the erodibility. The compaction water content also has a strong influence with steep gradients in the change of k_d on the dry side of optimum and less influence with flatter gradients of change on the wet side of optimum.

The other parameter that is influenced by compaction is τ_c. Hanson and Hunt (2007) observed that τ_c tends to be inversely related to k_d. This behavior was also observed for the seven soils in table 1. Figure 13 shows the relationship of τ_c versus WC for Soil D (table 1) with the same compaction effort and soil as shown in figures 10 and 11.

It may be noted that the erodibility, or erosion resistance, for fine grained soils is influenced by, but is not strictly correlated to, clay percentage or plasticity. Compaction effort, compaction water content, and other complicating factors play a role in erodibility of soil materials. Therefore, tables 2 and 3 do not provide exact values, but rather a summary of expected values, of k_d and τ_c for ranges of clay content, wet and dry of optimum water content, and compaction effort. These tables provide values that may be used as initial estimates of material erodibility parameters for dam overtopping analysis in cases where measured values do not exist.

Total Unit Weight

The total unit weight, γ_t, is used in WinDAM B for the force balance analysis of the Hanson/Robinson headcut migration model (eq. 3) (Hanson et al., 2001). The γ_t value is determined based on the weight of soil particles and water within a specified volume (Lambe and Whitman, 1979). The anticipated range of total unit weight for soil materials is from 1.3 to 2.3 g cm^{-3}.

Table 1. Material properties.

Soil Sample	USCS Classification	Atterberg Limits: Liquid Limit (%)	Atterberg Limits: Plasticity Index (%)	Texture: % Sand > 0.074 mm	Texture: % Clay < 0.002 mm
A	SM	NP	NP	73	6
B	SM	NP	NP	64	9
C	ML	23	3	32	15
D	CL	26	15	35	25
E	CL	31	15	24	26
F	CL	37	19	20	28
G	CL	37	17	13	35

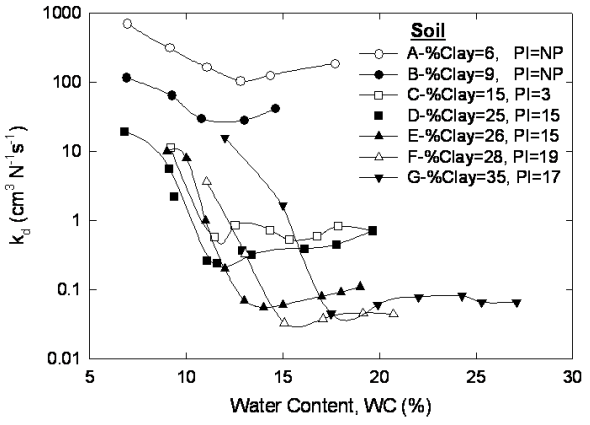

Figure 12. The detachment coefficient variation for seven soils at standard compaction effort of 6.0 kg cm cm^{-3} for range of water contents.

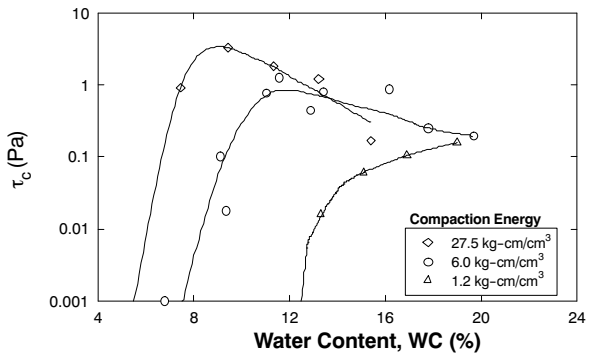

Figure 13. Variation of τ_c with compaction water content at three different compaction efforts.

Table 2. Approximate values of k_d (cm^3·N^{-1} s^{-1}) relative to compaction and % clay.

Clay (%)	Modified Compaction (27.5 kg-cm/cm^3) ≥Opt WC%	Modified Compaction (27.5 kg-cm/cm^3) <Opt WC%	Standard Compaction (6.0 kg-cm/cm^3) ≥Opt WC%	Standard Compaction (6.0 kg-cm/cm^3) <Opt WC%	Low Compaction (kg-cm/cm^3) ≥Opt WC%	Low Compaction (kg-cm/cm^3) <Opt WC%
>25	0.05	0.5	0.1	1	0.2	2
14-25	0.5	5	1	10	2	20
8-13	5	50	10	100	20	200
0-7	50	200	100	400	200	800

Table 3. Approximate values of τ_c (Pa) relative to compaction and % clay.

Clay (%)	Modified Compaction (27.5 kg-cm/cm^3)		Standard Compaction (6.0 kg-cm/cm^3)		Low Compaction (kg-cm/cm^3)	
	≥Opt WC%	<Opt WC%	≥Opt WC%	<Opt WC%	≥Opt WC%	<Opt WC%
>25	16	0.16	4	0.04	1	0.01
14-25	0.16	0.01	0.04	0	0.01	0
8-13	0.0	0	0	0	0	0
0-7	0	0	0	0	0	0

Unconfined Compressive Strength

WinDAM B uses the undrained shear strength, c_u, approximated by taking one half of the unconfined compressive strength, q_u, of the soil material, as input for predicting headcut migration rate in the force balance analysis to determine E_v in equation 3. ASTM D2166 provides a description of the testing methodology to determine the unconfined compressive strength of cohesive soil. Moore (1997) provided a table for estimating unconfined compressive strength for cohesive soils (table 4).

Headcut Migration Coefficient

The energy-based headcut advance model, designated the Temple/Hanson model on the WinDAM B input screens, computes headcut advance rate using equation 2. The material dependent constant, C, has been observed to vary over several orders of magnitude [0.01 to 30 (cm h^{-1}) (cm s$^{-1/3}$)$^{-1}$] and is affected by compaction energy, water content, density, and material type (Hanson et al., 2005a). For the headcut migration tests described by Hanson et al. (2001) a C value and a k_d value were determined for each test. Figure 14 shows the relationship between the C and k_d values from these tests. This relationship, C equal to approximately one-fourth k_d for the units indicated, may be used to estimate C from measured k_d values or those given in table 2.

Application

The embankment breach portion of WinDAM B is an adaptation/expansion of the technology tested in the SIMBA (Simplified Breach Analysis) research model (Temple et al., 2005; Hanson et al., 2005b; Tejral et al., 2009) for application to field conditions. This technology is primarily applicable to homogeneous embankment dams constructed from cohesive soil materials. Inputs required for application of this component are a simplified embankment cross section, the properties of the embankment material, the variation of the crest elevation along the length of dam, and the properties of any vegetal or riprap protection on the downstream face.

Outputs from the embankment breach component include the breach initiation time (end of stage 2), breach formation time (end of stage 3), and plots of the progressive erosion. The inflow and outflow hydrographs are provided in graphical and tabular format with plots of reservoir water surface and tailwater elevations versus time. The tabular listing of the outflow hydrograph, including predicted breach outflow, may be used as input to other flood routing software to predict downstream conditions.

Of the seven embankment overtopping tests conducted by Hanson et al. (2005a) tests 1 and 2 are presented here as examples of application of WinDAM B in predicting breach characteristics. The embankment dimensions were the same for both tests: 2.3-m height, 3 to 1 upstream and downstream slopes, 1.8-m wide crest, and 7.3-m wide test section. Each test embankment (fig. 1a) had a constructed notch that was 0.46-m deep and 1.8-m wide at the base with 3 to 1 side slopes to control the initial overtopping flow.

Embankment Test 1

Embankment test 1was constructed of a non-plastic silty loam with 70% sand and 5% clay. The measured soil parameters for these tests were: 1) k_d and τ_c values based on JET results of 10.2 cm^3 N^{-1} s^{-1} and 0 Pa, respectively; 2) total unit weight, γ_t, of 1.87 g cm-^{3}; and 3) undrained shear strength, c_u, of 10 kPa. These material properties were input to WinDAM B along with the embankment cross section, the variation of the crest elevation along the length of dam, the properties of the vegetal condition on the downstream face,

Table 4. Undrained shear strength for cohesive soil (Moore, 1997).[a]

Consistency	Field Identification Tests[b]	SPT (Blows/0.3 m)	q_u, Unconfined Compressive Strength (kPA)[c]	$C_u = 1/2 q_u$ Undrained Shear Strength (kPa)
Very soft	Exudes between fingers when squeezed in hand	<2	<40	<20
Soft	Easily molded with fingers, point of geologic pick easily pushed into shaft of handle	2–4	40-80	20-40
Firm	Penetrated several cm by thumb with moderate pressure. Molded by fingers with some pressure.	4-8	80-150	40-75
Stiff	Indented by thumb with great effort. Point of geologic pick can be pushed in up to 1 cm. Very difficult to mold with fingers. Just penetrated with hand spade.	8-15	150-300	75-150
Very stiff	Indented only by thumbnail. Slight indentation by pushing point of geologic pick. Requires hand pick for excavation.	15-30	300-625	150-313

[a] If the anticipated water content is unknown cohesive soils should be evaluated in the saturated condition. For non-cohesive soils or NP soils for which q_u is unknown, a value of $C_u = 0$ should be assumed.
[b] SPT - Standard Penetration Test (ASDM D-1586).
[c] kPa = 20.9 psf.

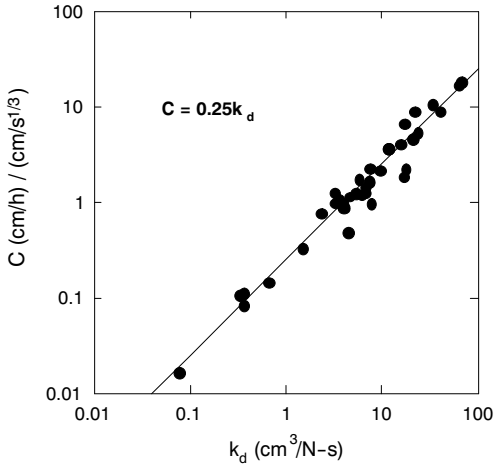

Figure 14. Relationship of C and K_d determined from flume tests.

the reservoir elevation and storage relations, and the inflow hydrograph. The WinDAM B breach discharge hydrograph, along with the measured inflow and breach hydrograph, for embankment test 1 is shown in figure 15a. The predicted timing, shape, and discharge are very close to the measured values.

EMBANKMENT TEST 2

Embankment test 2was constructed of a clay loam material with 25% sand and 26% clay. The measured soil parameters for this test were: 1) k_d and τ_c values based on JET results of 0.04 cm^3 N^{-1} s^{-1} and 14 Pa, respectively; 2) total unit weight, γ_t, equal to 1.92 g cm^{-3}; and 3) undrained shear strength, c_u, of 34 kPa. These material properties were input to WinDAM B along with the embankment cross section, the variation of the crest elevation along the length of dam, the properties of the vegetal condition on the downstream face, the reservoir elevation and storage relations, and the inflow hydrograph. The WinDAM B breach discharge hydrograph, along with the measured inflow and breach hydrograph, for embankment test 2 is shown in figure 15b. As can be noted, this test did not breach in the 20 h of testing. The predicted timing, shape, and discharge are very close to the measured values.

SUMMARY

Windows Dam Analysis Modules B (WinDAM B) is a modular software application, currently in test status, as a simplified computational model representing the observed erosion processes leading to embankment breach. The computational model incorporated into this software is the result of erosion process and erosion rate research that include embankment overtopping tests conducted in the outdoor laboratory. The components of the breach erosion modeling portion of WinDAM B are based on the four stages of observed breach development. The primary algorithms used in WinDAM B for predicting erosion are based on the excess stress equation and two headcut advance equations. For the model to be useful for field application, the algorithms have been developed to utilize soil parameters that may be reasonably obtained from field measurements or estimated from information provided here. This article presents the background for the material parameter input requirements for overtopping erosion and breach analysis including: 1) the detachment rate coefficient, k_d, and critical stress, τ_c,parameters of the excess stress equation; 2) the total unit weight, γ_t, of soil; 3) the undrained shear strength, c_u; and 4) the headcut advance coefficient, C.

The excess stress equation parameters, k_d and τ_c, measured using the JET are consistent with the large-scale erosion processes observed in the embankment breach. Therefore, the JET can be used to measure these required inputs to WinDAM B. Tables 2 and 3, constructed from JET tests on seven soils with a range of water content and compaction effort, may be used to estimate these parameters. However, the authors do recommend measuring erodibility. Estimates can be useful to conduct preliminary breach evaluations or when erodibility measurements are not available.

The total unit weight and undrained shear strength are used in WinDAM B for predicting headcut advance using the Hanson/Robinson model. Standard soil measurement methods are recommended for determining these values, but estimates can be useful to conduct preliminary breach evaluations or when measured values are not available. The headcut advance coefficient, *C*, is an input parameter if the Temple/Hanson model is used in breach model predictions. The authors recommend estimating the *C* value based on the relationship to the measured detachment rate coefficient k_d

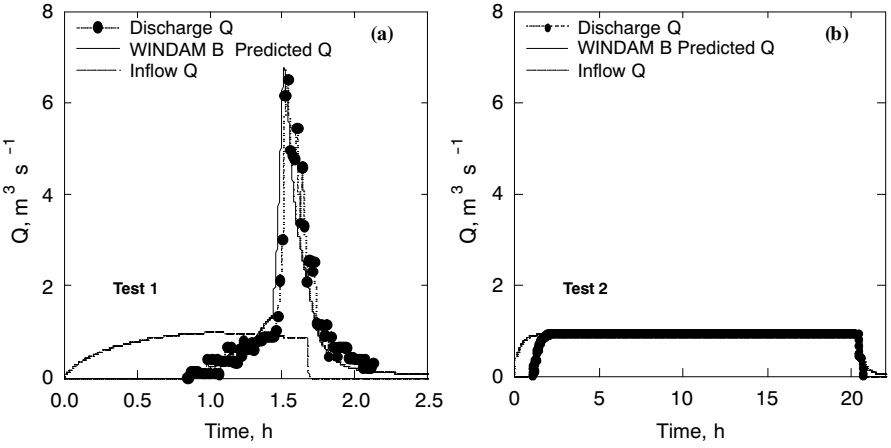

Figure 15. Observed inflow, discharge, and WinDAM B predicted discharge hydrographs for (a) overtopping test 1 and (b) overtopping test 2.

as described in this article. Data obtained from experience with similar embankment conditions and materials in the local area may also be used to estimate *C* when these data are available.

REFERENCES

Arulanandan, K., A. Sargunam, P. Loganathan, and R. B. Krone. 1973. Application of chemical and electrical parameters to prediction of erodibility. In *Soil Erosion: Causes and Mechanisms; Prevention and Control,* 42-51. Special Report 135: Highway Research Board. Washington, D.C.: HRB.

ASTM (American Society for Testing and Materials). 2010. Section 4. Constructing, Vols. 04.08 and 04.09. West Conshohocken, Pa.: ASTM.

Briaud, J. L., F. C. K. Ting, H. C. Chen, Y. Cao, S. W. Han, and K. W. Kwak. 2001. Erosion function apparatus for scour rate predictions. *ASCE J. Geotech. and Geoenv. Eng.* 127(2): 105-113.

Dillaha, T. A., and D. B. Beasley. 1983. Distributed parameter modeling of sediment movement and particle size distribution. *Trans. ASAE* 26(6): 1716-1722.

Foster, G. R., L. D. Meyer, and A. Onstad. 1977. An erosion equation derived from basic erosion principles. *Trans. ASAE* 20(4): 678-682.

Hanson, G. J. 1989. Channel erosion study of two compacted soils. *Trans. ASAE* 32(2): 485-490.

Hanson, G. J. 1990a. Surface erodibility of earthen channels at high stresses: Part I. Open channel testing. *Trans. ASAE* 33(1): 127-131.

Hanson, G. J. 1990b. Surface erodibility of earthen channels at high stresses: Part II. Developing an *in-situ* testing device. *Trans. ASAE* 33(1): 132-137.

Hanson, G. J., K. M. Robinson, and K. R. Cook. 2001. Prediction of headcut migration using a deterministic approach. *Trans. ASAE* 44(3): 525-531.

Hanson, G. J., K. M. Robinson, and K. R. Cook. 2002. Scour below an overfall: Part II. Investigation. *Trans. ASAE* 45(5): 957-964.

Hanson, G. J., and K. R. Cook. 2004. Apparatus, test procedures, and analytical methods to measure soil erodibility *in-situ*. *Applied Eng. in Agric.* 20(4): 455-462.

Hanson, G. J., K. R. Cook, and S. L. Hunt. 2005a. Physical modeling of overtopping erosion and breach formation of cohesive embankments. *Trans. ASAE* 48(5): 1783-1794.

Hanson, G. J., D. M. Temple, M. Morris, M. Hassan, and K. R. Cook. 2005b. Simplified breach analysis for homogeneous embankments: Part 2. Parameter inputs and variable scale model comparisons. *Proc. United States Society on Dams. Conf. Technologies to Enhance Dam Safety and the Environment,* 163-174. Denver, Colo.: USSD.

Hanson, G. J., and S. L. Hunt. 2007. Lessons learned using laboratory JET method to measure soil erodibility of compacted soils. *Applied Eng. in Agric.* 23(3): 305-312.

Hanson, G. J., S. L. Hunt, and D. M. Temple. 2010. Coherence of erodibility for erosion processes and different scales. In *Proc of the Joint Federal Interagency Sedimentation and Hydrologic Modeling Conference.* Las Vegas, Nev.: FISC.

Hassan, M., M. Morris, G. Hanson, and K. Lakhal. 2004. Breach formation: Laboratory and numerical modeling of breach formation. In *Proc. Dam Safety 2004.* Phoenix, Ariz.: ASDSO.

Hollick, M. 1976. Towards a routine test for the assessment of critical tractive forces of cohesive soils. *Trans. ASAE* 19(6): 1076-1081.

Hunt, S. L., G. J. Hanson, K. R. Cook, and K. C. Kadavy. 2005. Breach widening observations from earthen embankment tests. *Trans. ASAE* 48(3): 1115-1120.

Hutchinson, D. L. 1972. Physics of erosion of cohesive soils. Ph.D. thesis. Aukland, New Zealand: Univ. of Aukland.

Lambe, T. W., and R. V. Whitman. 1979. *Soil Mechanics, SI Version.* New York, N.Y.: J. Wiley & Sons.

Lim, S. S. 2006. Experimental investigation of erosion variably saturated clay soils. Ph.D. thesis. Australia: School of Civil and Environmental Engineering, the University of New South Wales.

Moore, J. S. 1997. Field procedures for the headcut erodibility index. *Trans. ASAE* 40(2): 425-336.

Moore, W. L., and F. D. Masch, 1962. Experiments on the scour resistance of cohesive sediments. *J. Geophysical Res.* 67(4): 1437-1446.

Mostafa, T. S., J. Imran, M. H. Chaudhry, and I. B. Kahn. 2008. Erosion resistance of cohesive soils. *J. Hydraulics Res.* 46(6): 777-787.

Partheniades, E., and R. E. Paaswell. 1968. Erosion of cohesive soil and channel stabilization. Civil Eng. Report No. 19. Buffalo, N.Y.: New York State University.

Ralston, D. C. 1987. Mechanics of embankment erosion during overflow. *Proc. 1987 National Conf. on Hydraulic Eng.*, 737-738. Reston, Va.: ASCE Hydraulics Div.

Smerdon, E. T., and R. P. Beasley. 1959. The tractive force theory applied to stability of open channels in cohesive soils. Research Bulletin 715. University of Missouri. Ag. Exp. Station.

Stein, O. R., and D. D. Nett, 1997. Impinging jet calibration of excess shear stress sediment detachment parameters. *Trans. ASAE* 40(6): 1573-1580.

Temple, D. M. 1985. Stability of grass-lined channels following mowing. *Trans. ASAE* 28(3): 750-754.

Temple, D. M., G. J. Hanson, M. L. Neilsen, and K. R. Cook. 2005. Simplified breach analysis for homogeneous embankments: Part 1. Background and model components. In *Proc. United States Society on Dams, Technologies to Enhance Dam Safety and the Environment,* 151-161. Denver, Colo.: USSD.

Terjal, R. D., G. J. Hanson, and D. M. Temple. 2009. Comparison of two process based earthen dam failure computation models. In *Proc. Dam Safety 2009,* Ft. Lauderdale, Fla.: ASDSO.

Vaskinn, K. A., A. Lovoll, K. Hoeg, M. Morris, and G. Hanson. 2004. Physical modeling of breach formation: Large scale field tests. In *Proc. Proc. Dam Safety 2004.* Phoenix, Ariz.: ASDSO

Wahl, T. L., G. J. Hanson, and P. L. Regazzoni. 2009. Quantifying erodibility of embankment materials for the modeling of dam breach processes. *Proc. Dam Safety 2009.* Ft. Lauderdale, Fla.: ASDSO.

Walder, J. S., and J. E. O'Connor. 1997. Methods of predicting peak discharge of floods caused by failure of natural and constructed dams. *Water Resources Res.* 33(10): 2337-2348.

Wan, C. F., and R. Fell. 2004. Investigation of rate of erosion of soils in embankment dams. *J. Geotech. and Geoenv. Eng.* 130(4): 373-380.